

Efficiency of excavations with buttress walls in reducing the deflection of the diaphragm wall

Pio-Go Hsieh¹ · Chang-Yu Ou² · Wei-Han Hsieh²

Received: 18 January 2015 / Accepted: 13 September 2015 / Published online: 19 November 2015
© Springer-Verlag Berlin Heidelberg 2015

Abstract Installation of buttress walls against diaphragm walls has been used as an alternative measure for the protection of adjacent buildings during excavation, but their mechanism in reducing movements has not yet been fully understood. This study performs three-dimensional finite element analyses of two excavation case histories, one in clay with T-shape buttress walls and another in dominant sand with rectangular buttress walls, to establish analysis model. Then, a series of parametric study were performed by varying soil types, types and length of buttress walls based on the above-mentioned excavations. Results show that the mechanism of buttress walls in reducing wall deflections mainly came from the frictional resistance between the side surface of buttress wall and adjacent soil rather than from the combined bending stiffness from diaphragm and buttress walls. The buttress wall with a length <2.0 m had a poor effect in reducing the wall deflection because the soil adjacent to the buttress wall had almost the same amount of movement as the buttress wall, causing the frictional resistance little mobilized. Since the frictional resistance of buttress walls in a deep excavation

has fully been mobilized prior to the final excavation depth, the efficiency of buttress walls in reducing the wall deflection in a deep excavation was much less than that in a shallow excavation. Rectangular shape of buttress walls was of a better effect than T-shape in the shallow excavation because frictional resistance between buttress walls and adjacent soil played a major role in reducing the wall deflection rather than bearing resistance of the flange. When the excavation went deeper, the difference in reducing the wall deflection between the R-shape and T-shape became small.

Keywords Buttress wall · Deep excavation · Shallow excavation · Wall deflection

1 Introduction

Deep excavation may induce excessive wall deflections and ground settlements and thus damage adjacent buildings. To avoid the damage of adjacent buildings during excavation, it is necessary to adopt effective measures to limit the wall deflection or ground settlement. Ground improvement is a common measure to reduce the excavation-induced ground movements [8, 18, 25, 29]. Recently, cross walls, constructed perpendicularly and connected to the two opposite diaphragm wall, have been widely used in some countries as an alternative measure. The authors have shown that use of cross walls in deep excavations can reduce the wall deflection to a very small amount [11, 23, 24]. However, use of cross walls in a very wide excavation would be costly. Therefore, buttress walls have been adopted recently as an alternative to cross walls for the protection of adjacent buildings during deep excavation [4, 9, 10, 12, 13].

✉ Chang-Yu Ou
ou@mail.ntust.edu.tw

Pio-Go Hsieh
spg@cc.hwh.edu.tw

Wei-Han Hsieh
ufo.9876@gmail.com

¹ Department of Assets and Property Management, Hwa Hsia University of Technology, 111, Gongzhuan Rd., Zhonghe Dist., New Taipei City 23568, Taiwan

² Department of Civil and Construction Engineering, National Taiwan University of Science and Technology, 43, Sec. 4, Keelung Rd, Taipei 10672, Taiwan

The basic configuration of a buttress wall is depicted in Fig. 1. A buttress wall is similar to a cross wall in terms of construction. It is a concrete wall perpendicular to the diaphragm wall constructed before excavation, but not connected to the opposite diaphragm wall. Conceptually, a buttress wall may provide frictional resistance developing on the two sides of the buttress wall and thus increase the overall lateral resistance against the movement of the diaphragm wall during excavation. It may also function like a T-beam as that in reinforced concrete structures, enhancing the capability of moment resistance of the diaphragm wall. No matter which mechanism of buttress walls exists in deep excavations, the wall movement is expected to reduce to a certain extent.

According to the experiences of practicing engineers, buttress walls seem to have a good effect in reducing the movement of diaphragm walls though their effectiveness and mechanism are not yet verified [10]. Buttress walls are thus gradually popular in reducing excavation-induced movements in some Asian countries in recent years. Moreover, although buttress walls have been applied in many deep excavations, research on their behavior is rather deficient. Only a few studies on buttress walls have been found in the literature. For example, Hsieh and Lu [9] introduced a preliminary design method for a buttress wall, and Hwang et al. [13] investigated the behavior of the buttress wall. Chen et al. [4] examined the influence of the geometry of the buttress walls (shape, thickness, and length) on the displacement of buttressed diaphragm wall by performing three-dimensional finite element analysis. The mechanism of buttress walls in reducing the deformation of diaphragm wall remains resolved.

In this paper, two excavation cases with buttress walls, one with T-shape buttress walls in clay and the other with rectangular shape buttress walls, referred to as R-shape, in predominating sandy soil, were analyzed using the three-

dimensional finite element method. The buttress walls in both cases were demolished along with excavation. The rationality of analysis results was validated by the comparison between the monitoring data and analysis results. Characteristics of wall deflection and development of lateral resistance from buttress walls were further studied using the three-dimensional finite element method by varying the length, shape and soil properties in these two cases.

2 Finite element analysis and constitutive model

A three-dimensional finite element computer program, PLAXIS 3D [26], was used as a basic analysis tool. The Hardening Soil model [28], referred to as the HS model, was adopted for analysis. In addition to the strength parameters (c' , ϕ'), the HS model requires the other seven parameters, namely ψ , E_{50}^{ref} , $E_{\text{oad}}^{\text{ref}}$, $E_{\text{ur}}^{\text{ref}}$, m , R_f and ν_{ur} , to describe the stress–strain behavior of soil. Table 1 lists the parameters, their definition and the way of evaluating their values in this study. As shown in this table, the way of determining the stiffness parameters of sandy and clayey soils was different. According to the relations listed in Table 1, the unloading/reloading referential stiffness ($E_{\text{ur}}^{\text{ref}}$) of clayey soil was evaluated first based on the initial void ratio (e) and the swelling index (C_s) that were little influenced by the possible disturbance of soil sampling process. Then estimate the referential secant stiffness (E_{50}^{ref}) followed by the evaluation of the referential oedometer stiffness ($E_{\text{oad}}^{\text{ref}}$). For sandy soil, the Young's modulus (E_s) of in situ soil was estimated first according to the relationship of $E_s \approx (2000 \sim 3000)N$ that was obtained by back-analyzing excavation cases in sandy soil, where N is the standard penetration number [15]. Then estimate the E_{50}^{ref} followed by the evaluation of the $E_{\text{oad}}^{\text{ref}}$ and $E_{\text{ur}}^{\text{ref}}$

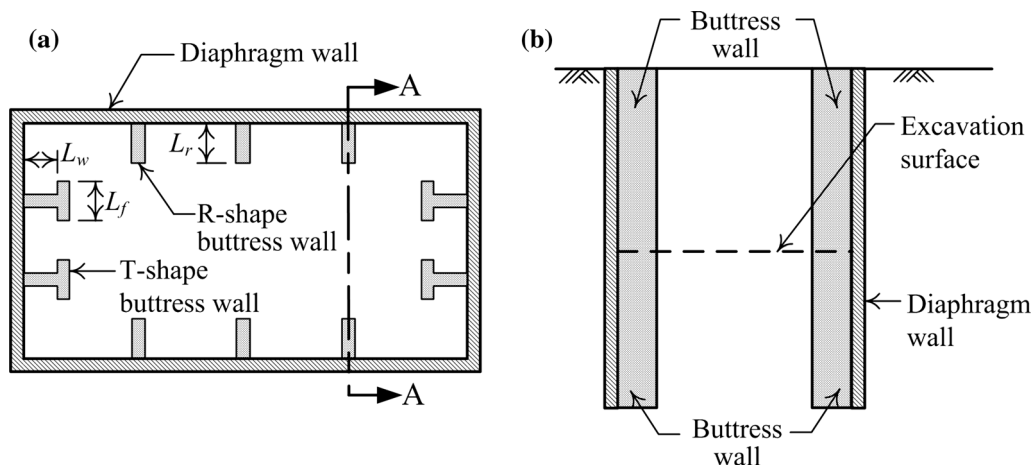


Fig. 1 Schematic diagram of the buttress wall **a** plan; **b** A–A section

Table 1 Parameters of the HS model

	Physical implication	Method of evaluation	References
ψ	The angle of dilatancy	$\psi = \phi' - 30^\circ$	Bolton [2]
E_{50}^{ref}	The referential secant stiffness in primary loading	$E_{50}^{\text{ref}} = E_{\text{ur}}^{\text{ref}}/3$ for clay $E_{50}^{\text{ref}} = E_s / [3(\sigma'_3/p^{\text{ref}})^m]$ for sand	Calvello and Finno [3] Khoiri and Ou [15]
$E_{\text{oed}}^{\text{ref}}$	The referential tangent referential stiffness in primary oedometer loading	$E_{\text{oed}}^{\text{ref}} = 0.7E_{50}^{\text{ref}}$ for clay $E_{\text{oed}}^{\text{ref}} = 1.5E_{50}^{\text{ref}}$ for sand	Calvello and Finno [3], Khoiri and Ou [15]
$E_{\text{ur}}^{\text{ref}}$	The referential unloading/reloading stiffness	$E_{\text{ur}}^{\text{ref}} = \frac{3(1+e)p^{\text{ref}}(1-2\nu_{\text{ur}})}{C_v/\ln 10}$ for clay $E_{\text{ur}}^{\text{ref}} = 3E_{50}^{\text{ref}}$ for sand	Lim et al. [17] Khoiri and Ou [15]
m	The power for stress-level dependency of stiffness	$m = 1.0$ for clay $m = 0.5$ for sand	Schanz et al. [28]
R_f	The ratio of the asymptotic strength to the failure strength	0.9	Duncan and Chang [7], Schanz et al. [28]
ν_{ur}	The Poisson's ratio in the unloading–reloading state	0.2	–

The referential pressure $p^{\text{ref}} = 100$ kPa

according to the correlations listed in Table 1. Moreover, the silty gravel soil exists in the Taipei Basin around 45 m below the ground surface and its stiffness parameters, back-analyzed by Deng [6] through back analysis, that the $E_{\text{ur}}^{\text{ref}}$, E_{50}^{ref} and $E_{\text{oed}}^{\text{ref}}$ were about equal to 256, 85 and 85 MPa, respectively.

Installation of diaphragm wall and buttress wall and their construction quality may affect the stress redistribution of the soil [5, 19, 27], and numerical analysis may not exactly simulate all the installation effects. For simplifying analysis, the diaphragm wall was assumed to be wished in place and the soil before excavation was in the at-rest state but the weight of the concrete from D-wall and buttress wall over the existing soil was applied to the soil. The coefficient of the at-rest earth pressure for sandy soil (K_0) can be obtained by the equation $K_0 = 1 - \sin\phi'$ [14]. The $K_{0,\text{OC}}$ value for clay can be obtained according to Ladd et al. [16] as

$$K_{0,\text{OC}} = K_{0,\text{NC}}(\text{OCR})^\alpha \quad (1)$$

where $K_{0,\text{OC}}$ is the at-rest earth pressure coefficient at the overconsolidated state, and $K_{0,\text{NC}}$ is that at the normally consolidated state, OCR is the overconsolidated ratio, and α is an empirical coefficient and can be approximated by $\alpha = \sin\phi'$.

The structural members such as diaphragm walls, buttress walls and concrete floor slabs employed in the top-down construction method were with plate elements and simulated as linear elastic material. The Poisson's ratio for concrete is set equal to 0.15. The Young's modulus of concrete was estimated using the equation $E_c = 4700\sqrt{f'_c}$, where f'_c is the compressive strength of concrete (MPa) [1]. In analysis, the E_c of concrete was reduced by 20 %, considering that cracks may appear in the diaphragm wall when

it is subject to a large deflection [22], which is also an overall effect of assumption of linear elastic behavior of material. The temporary struts were with axial elements and also simulated as linear elastic material. The axial stiffness of the struts was reduced by about 50 %, considering possible defects of alignment of struts in the field [22].

The interaction between the wall and soil was simulated with interface elements, whose behavior follows the Mohr–Coulomb model. In this study, the friction angles of interface elements were set the same as soil.

It should be noted that the parameters of soils and structural members in the following case studies were evaluated preliminarily according to the above description. Except for the K_0 values, the parameters were also calibrated at the early stages of excavation based on the monitored wall deflections, especially those correlations given in a range.

3 Case studies

3.1 The Park-2001 project

The Park-2001 project was a 44 by 42 m excavation located in Taipei. The diaphragm wall was 21 m in depth and 0.6 m in thickness. In order to protect a gas station near the excavation, three T-shape buttress walls, with the thickness (t_{bw}) of 0.6 m, the flange length (L_f) of 2.5 m and web length (L_w) of 5 m, were constructed from the 2.0 m below the ground surface level (GL –2.0 m) to GL –22.0 m against the diaphragm wall as shown in Fig. 2a, b. Four excavation stages were conducted to reach the final depth of 8.6 m. Three levels of struts were employed to support the diaphragm wall, in which the first strut level

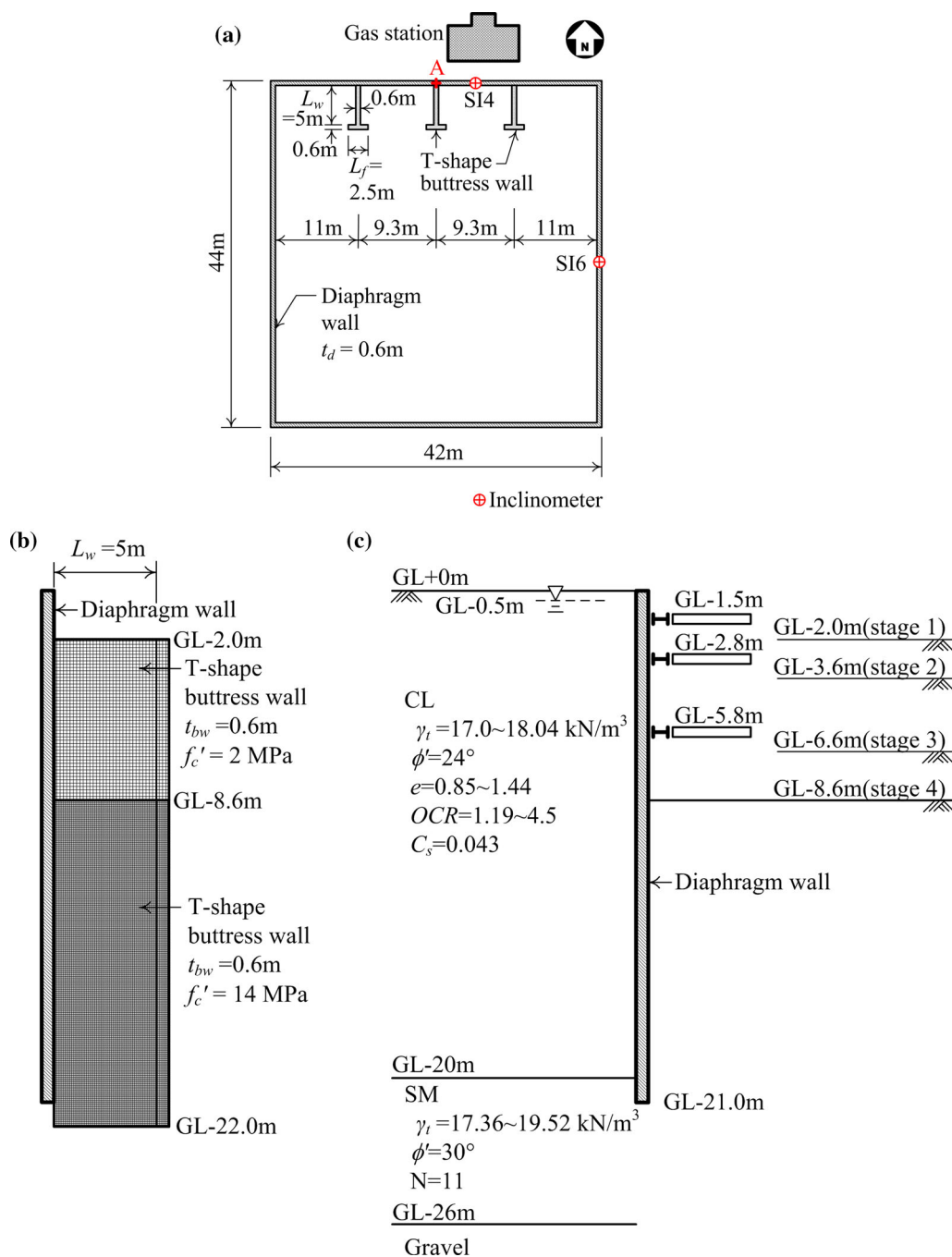


Fig. 2 Park-2001 excavation project **a** excavation geometry and instrumentation; **b** types of buttress wall; **c** profile of the subsurface soil and construction sequence

was $H330 \times 330 \times 10 \times 15$ while the second and third strut levels were $H400 \times 400 \times 13 \times 21$. The average horizontal spacing between struts was 6.0 m in the east–west direction and 5.5 m in the north–south direction. Figure 2c shows the construction sequence of excavation.

As shown in Fig. 2c, the silty clay locates from ground surface level to GL -20 m, in which the total unit weight ranges from 17.0 to 18.04 kN/m^3 , SPT-N value ranges

from 1 to 4, the water content ranges from 30 to 50 %, the liquid limit ranges from 37 to 50, and the plastic limit ranges from 21 to 26. The silty sand locates from GL -20 to GL -26 m with the total unit weight ranging from 17.36 to 19.52 kN/m^3 , and the SPT-N about 11. In addition, the ground water level is at 0.5 m below the ground surface. Two inclinometers, SI4 and SI6, were installed to observe wall deflection during excavation, as shown in Fig. 2a.

Figure 3 shows the finite element mesh used for analysis where the fine mesh as defined by PLAXIS was used, as suggested by Ou et al. [21]. The depth of the model was set at 26 m where hard rock exists. The horizontal boundaries were located at the distance two times the final excavation depth from the diaphragm wall as suggested by Ou and Shiau [20].

The parameters of the sand and clay at the construction site were determined in a way as shown in Table 1 and as the description in the preceding sections. Furthermore, the parameters of the soils and structure were calibrated at the earlier stages of excavation, and therefore, the lower bound of the correlation between the E_s and SPT-N for sandy soil was adopted for analysis. Table 2 summarizes the parameters of the soils used in the analysis where the clayey soil and sandy soil were assumed to be undrained and drained material, respectively. The analysis followed the construction procedure as shown in Fig. 2c.

Figure 4 plots a comparison of the computed and monitored wall deflections at SI4, near the location of a buttress wall. It can be observed that the computed wall deflections were in general close to the monitored values but slightly overestimated at the last two stages. For evaluating the effectiveness of buttress walls in reducing the wall deflection, analysis of the excavation with assumption of no buttress walls was performed and the results are also shown in Fig. 4. For global evaluation of the efficiency of buttress walls, the wall deflection at different sections along the diaphragm wall at a depth of final excavation bottom, usually close to the maximum value, is shown in Fig. 5. It can be found that the wall deflections were reduced significantly due to the installation of buttress walls. The computed maximum wall deflections with buttress wall and without buttress walls were 76.1 and 41.5 mm, respectively.

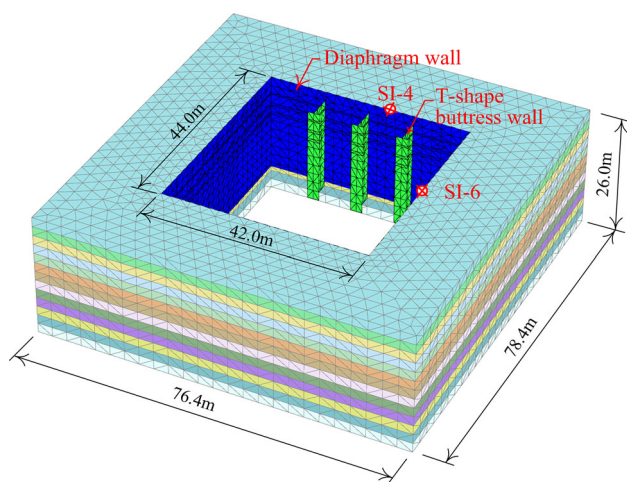


Fig. 3 Finite element mesh used for the Park-2001 excavation project

For evaluating the effectiveness of buttress walls in excavations quantitatively, the ratio of reduction in the maximum wall deflection (MR) is defined as

$$MR = \frac{\delta_{hm,nobw} - \delta_{h,bw}}{\delta_{hm,nobw}} \times 100\% \quad (2)$$

where $\delta_{hm,nobw}$ is the maximum deflection of the diaphragm wall with the assumption of no buttress walls installed, $\delta_{h,bw}$ is the deflection of the diaphragm wall, with buttress walls, at a depth corresponding to the maximum deflection of diaphragm wall without buttress walls.

As shown in Fig. 4, the MR value was 45.5 % at the final excavation stage. Installation of buttress walls can reduce the maximum wall deflection significantly.

3.2 The Jinshan south road project

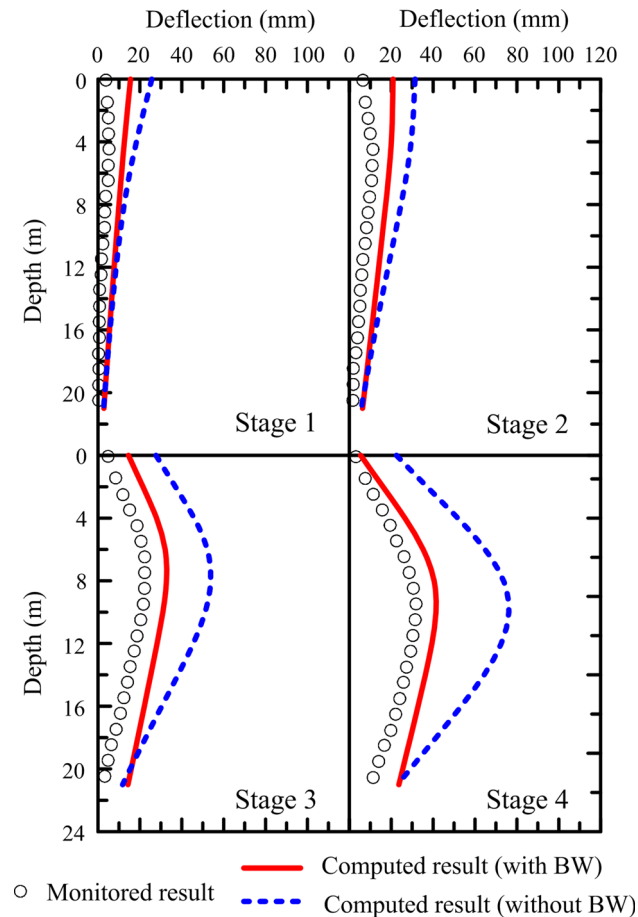
The Jinshan south road project was an 18-story building with 7-level basements locating in Taipei. As shown in Fig. 6a, the excavation was 64 m in length and 43 m in width, and surrounded by five buildings. The diaphragm wall was 43 m in depth and 1.3 m in thickness, penetrating 3.9 m into gravel layer. Three types of R-shape buttress walls with different t_{bw} and length (L_t) were installed as shown in Fig. 7, and their allocations are shown in Fig. 6a. The basement was constructed with the top-down construction method up to 26.45 m in depth. To monitor the wall deflection, seven inclinometers were installed penetrating 5 m into gravel layer. Among them, inclinometer SI1 was damaged at the beginning of excavation so their data were excluded in this study. Inclinometers SI3 and SI4 remained functional until stage 8, and the monitored values at all stages except for stage 8 were employed for study.

Figure 6b shows that the subsoil is comprised of seven alternating layers of clayey and sandy soils, among which the second and fourth layers of soils mainly affect the wall deflection. These layers are medium dense silty sand (SM) with friction angle about 30° . The SPT-N value, on the other hand, ranges from 5 to 17 for the second layer and from 22 to 27 for the fourth layer.

As shown in Fig. 6b, the soil was excavated, along with the demolition of buttress walls, to GL -2.5 m, referred to as stage 1. The concrete floor slab at the ground level (1FL) was then installed, and the soil and buttress walls were excavated and demolished, respectively, down to GL -5.45 m, referred to as stage 2. The procedure repeated until B5FL was installed, and soil and buttress walls were excavated and demolished, respectively, down to GL -20.2 m (stage 7). After completion of stage 7, the concrete floor slab was constructed at GL -18.60 m (B6FL) and the soil was excavated to the final depth, GL -26.45 m, but the buttress walls stayed at the same depth, no demolition, at this stage, referred to as stage 8. At

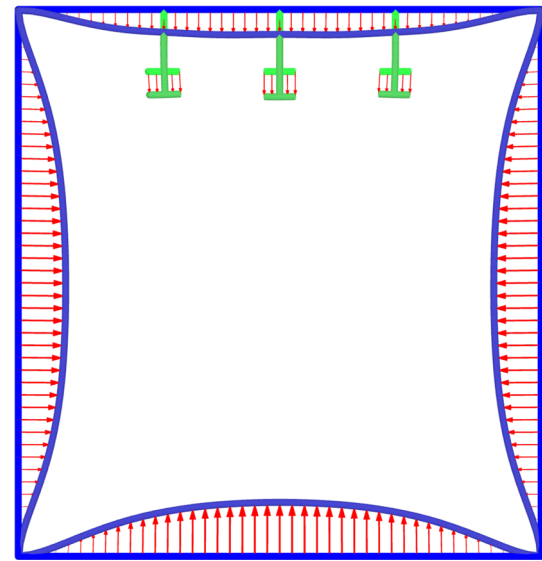
Table 2 Parameters of the HS model used in the Park-2001 project

Depth (m)	Soil type	Drainage type	γ_t (kN/m ³)	c' (kPa)	ϕ' (°)	ψ (°)	E_{ur}^{ref} (kPa)	E_{50}^{ref} (kPa)	E_{oed}^{ref} (kPa)	m	ν_{ur}
0–20	CL	Undrained	17.00–18.04	0	24	0	17,832–23,518	5944–7839	4161–5488	1.0	0.2
20–26	SM	Drained	17.36–19.52	0	30	0	22,012–24,101	7337–8034	11,006–12,050	0.5	0.2

**Fig. 4** Comparison of monitored and computed wall deflections at SI4 at all stages for the Park-2001 excavation project

stage 9, the final stage, a 0.9-m-thick mat foundation was cast at the final depth, i.e., GL –26.45 m, and then the buttress walls were demolished down to the final depth and the concrete floor slab (B7FL) was built. It should be noted that the concrete floor slabs 1FL, B1FL and B7FL were 0.25 m in thickness while the rest of slabs 0.4 m.

In finite element analysis, sandy and clayey soils were treated as drained and undrained material, respectively. The void ratio and swelling index of the soils were obtained directly from laboratory tests. Similar to the Park-2001 project, stiffness parameters of the gravel soil, locating below GL –39.6 m, were: $E_{ur}^{ref} = 256$ MPa, $E_{50}^{ref} = 85$ MPa and $E_{oed}^{ref} = 85$ MPa. The parameters of the soils were determined in a way as shown in Table 1 and

**Fig. 5** Wall deflection at different sections along the diaphragm wall at a depth of the excavation bottom for the Park-2001 excavation project

calibrated in a way similar to the preceding case. Table 3 summarizes the soil parameters used in this study.

Figure 8 shows the finite element mesh for the Jinshan south road project. The depth of mesh was set at GL –54.9 m, considering that hard rock would not deform during excavation. The horizontal boundaries were located at the distance two times the final excavation depth from the diaphragm wall. The finite element model was therefore 169.8 m in length and 148.8 m in width. The analysis followed the construction procedure as shown in Fig. 6b, including the weight of surrounding buildings and the depth of foundation, up to stage 8 because of no monitored data afterward.

Figure 9 shows a comparison of monitored and computed wall deflection at stage 8. For evaluation of the effectiveness of installation of buttress walls, analysis of the excavation with assumption of no buttress walls installed was also performed and the results are shown in the same figure. Moreover, the wall deflections at different sections along the diaphragm wall at a depth of final excavation bottom, usually close to the maximum value, are shown in Fig. 10. Despite no monitored wall deflections at SI3 and SI4 at stage 8, the monitored data before stage 8 were still used for validation and the computed wall

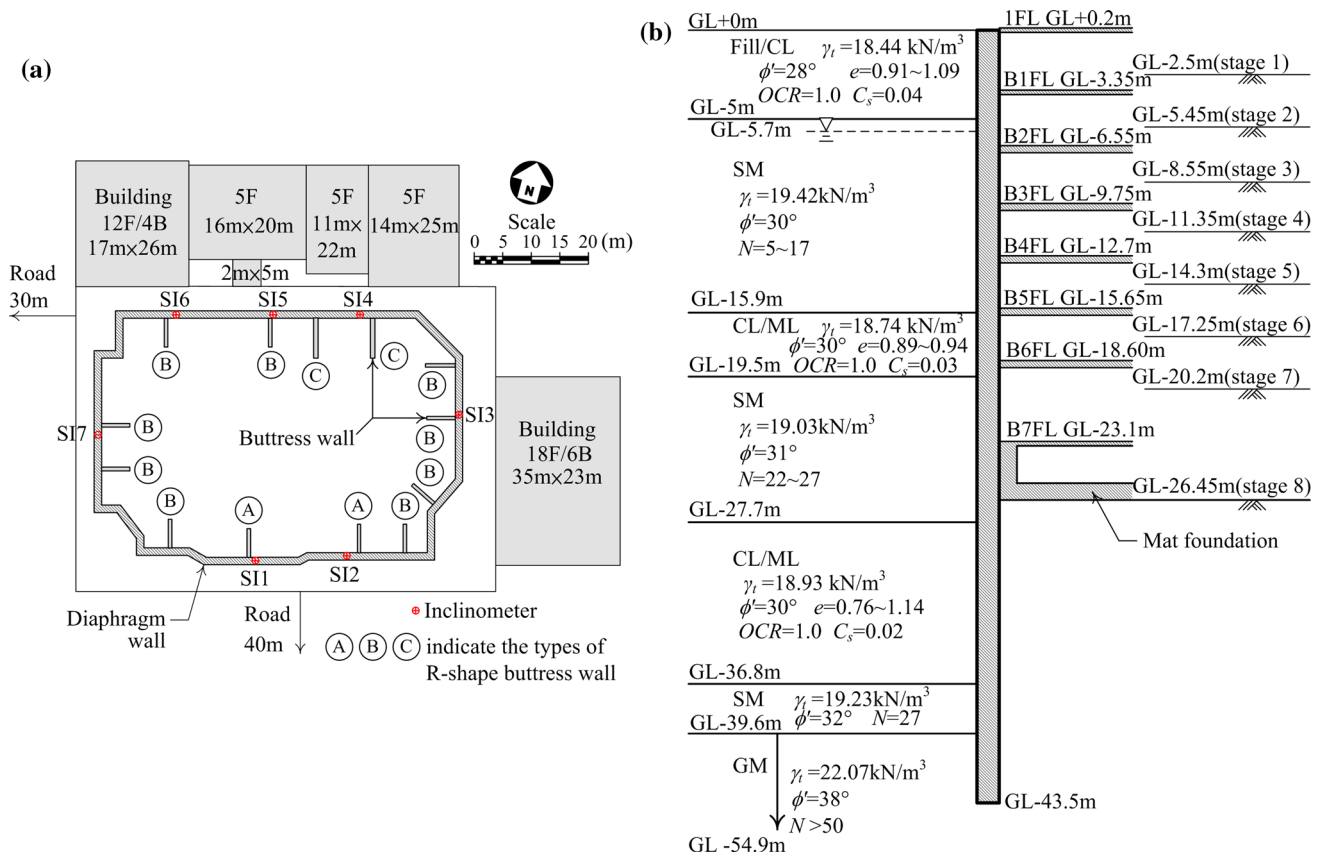


Fig. 6 Jinshan south road project **a** excavation geometry and instrumentation; **b** profile of the subsurface soil and construction sequence

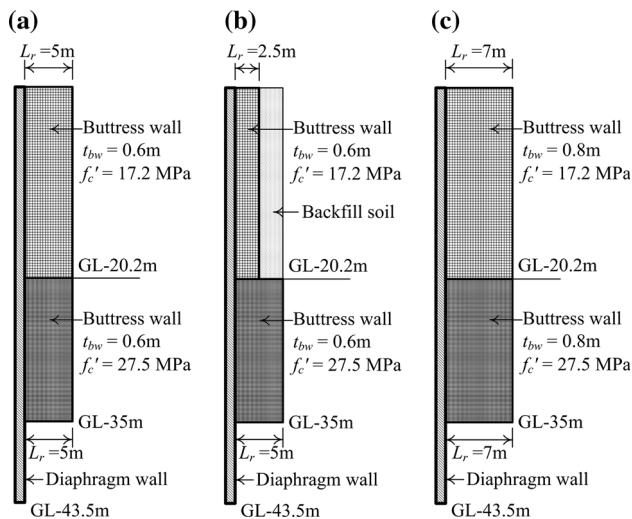


Fig. 7 Types of R-shape buttress walls used in the Jinshan south road project **a** type A; **b** type B; **c** type C

deflections at stage 8 were also used for studying the effectiveness of installation of buttress walls.

The computed wall deflections generally agreed with the monitored data for SI2, SI5, SI6 and SI7 at all excavation stages, and the comparison at stage 8 is shown in Fig. 9.

The agreement for SI3 and SI4 was also quite well from beginning up to stage 7 though their comparison was not shown here. The analysis validates the constitutive model adopted and analysis procedure in this study.

Figure 9 also shows that the wall deflections at SI2, SI3, SI4 and SI6 were slightly smaller than those without buttress walls. Their MR values were equal to 17.5, 17.4, 18.2 and 17.0 %, respectively. Installation of buttress walls had some effects in reducing the wall deflection. The wall deflections at SI5 and SI7 with buttress walls were moderately smaller than that without buttress walls. Their MR values were 26.9 and 23.9 %, respectively. Installation of buttress walls had a moderate effect in reducing the wall deflection.

4 Factors affecting the deflection of diaphragm wall with buttress walls

The above-mentioned two case histories were with different excavation depths, soil types, types and length of buttress walls, as summarized in Table 4. As indexed by the MR values, the Park-2001 project obviously had a better effect in reducing the wall deflection. Does it imply that

Table 3 Parameters of the HS model used in the Jinshan south road project

Depth (m)	Soil type	Drainage type	γ_t (kN/m ³)	c' (kPa)	ϕ' (°)	ψ (°)	E_{ur}^{ref} (kPa)	E_{50}^{ref} (kPa)	E_{oed}^{ref} (kPa)	m	v_{ur}
0–5	CL	Undrained	18.44	0	28	0	19,794–21,660	6598–7220	4619–5054	1.0	0.2
5–15.9	SM	Drained	19.42	0	30	0	15,543–40,573	5181–13,524	7771–20,287	0.5	0.2
15.9–19.5	CL/ML	Undrained	18.74	0	30	0	26,116–26,807	8705–8936	6094–6255	1.0	0.2
19.5–27.7	SM	Drained	19.03	0	31	1	43,880–48,621	14,627–16,207	21,940–24,311	0.5	0.2
27.7–36.8	CL/ML	Undrained	18.93	0	30	0	36,480–44,356	12,160–14,785	8512–10,350	1.0	0.2
36.8–39.6	SM	Drained	19.23	0	32	2	43,864	14,621	21,932	0.5	0.2
39.6–54.9	GM	Drained	22.07	0	38	8	256,000	85,000	85,000	0.5	0.2

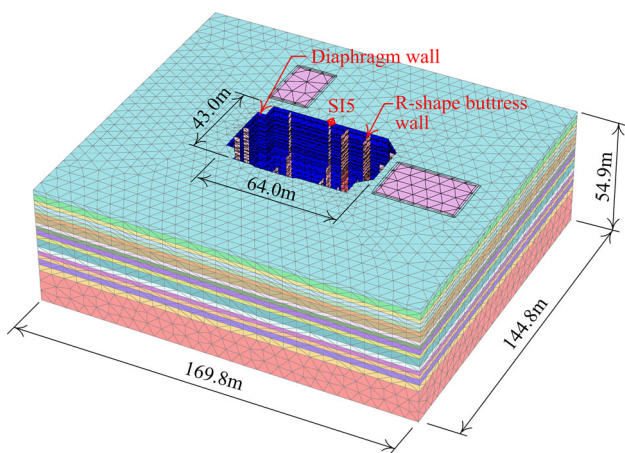


Fig. 8 Finite element mesh used for the Jinshan south road excavation project

buttress walls in the shallow excavations, and/or with dominating clay layer and/or with T-shape had a better restraining effect than those in the deep excavation, and/or with dominating sandy soil layer and/or with R-shape?

To clarify the queries, a series of three-dimensional finite element analyses were performed where the excavation geometry and construction sequence of the Park-2001 project and the Jinshan south road project, denoted as “shallow excavation” and “deep excavation”, respectively, were used as a basis, combined with different soil types, length and types of buttress walls. The soil profile as shown in Fig. 2b was treated as the “clay” type of the subsoil in the shallow excavation, while the soil profile as illustrated in Fig. 6b was regarded as the “sand” type of subsoil in the deep excavation. In addition, Fig. 11a, b shows the “sand” types of the subsurface soil profile in the shallow excavation and the “clay” type in the deep excavation, respectively. The construction of the shallow excavation was exactly the same as shown in Fig. 2b, while the construction sequence of the deep excavation was similar to that shown in Fig. 6b except for stage 8 where

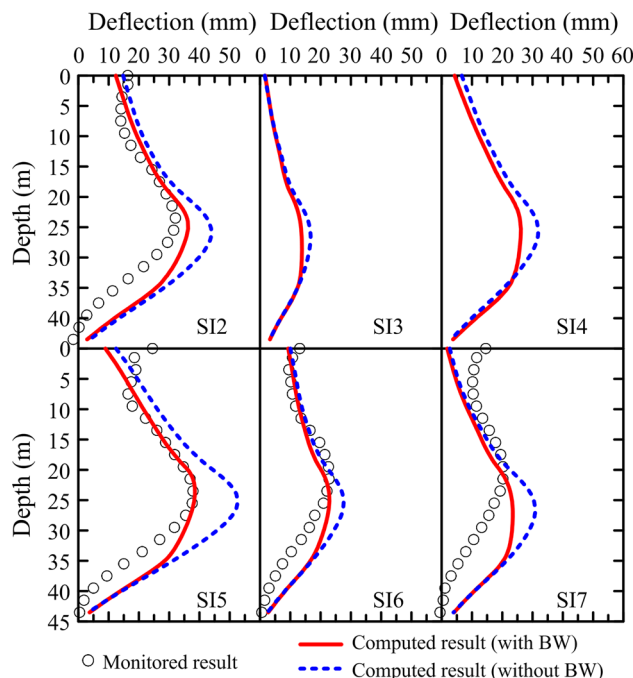


Fig. 9 Comparison of monitored and computed wall deflections at stage 8 for the Jinshan south road excavation project

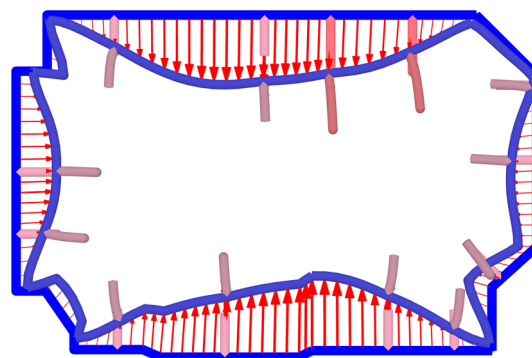


Fig. 10 Wall deflection at different sections along the diaphragm wall at a depth of the excavation bottom for the Jinshan south road excavation project

Table 4 Comparison of excavation condition, buttress wall type and dimension, and wall deflection between the Park-2001 and Jinshan south road excavation projects

Case	Park-2001	Jinshan
Excavation depth (m)	8.6	26.45
Excavation type	Shallow excavation	Deep excavation
Soil layer	Clayey soil	Sandy soil
Buttress wall type	T-shape	R-shape
L_r (m)	–	2.5–7
L_w, L_f (m)	5, 2.5	–
t_{bw} (m)	0.6	0.6
$\delta_{hm,bw}$ (mm)	41.5–40.6	13.8–38.5
$\delta_{hm,nobw}$ (mm)	76.1–79.0	16.7–52.7
MR (%)	45.5–48.6	17.0–26.9

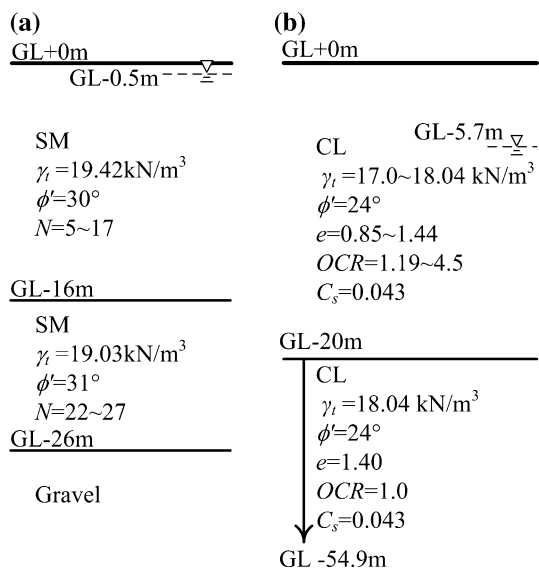


Fig. 11 Profile of subsurface soil layers **a** the sandy soil in the shallow excavation; **b** the clayey soil layer in the deep excavation

the buttress walls from GL –20.20 to GL –26.45 m were demolished with excavation of soil.

As referred to the dimension in Fig. 1, the T-shape buttress walls were with different dimensions: $L_w = 5\text{--}7.5$ m, $L_f = 2.5\text{--}5$ m while R-shape: $L_r = 5\text{--}20$ m. Analysis of each case with assumption of no buttress walls was also performed, and the resulting wall deflection at the same location was used for comparison.

The wall deflection and shear stress along the side surface of the buttress wall at point A in Fig. 2a and SI5 in Fig. 6a, both locating at about central section of the excavation, were employed for studying the reduction in wall deflection.

4.1 Mechanism of buttress walls in the reduction in wall deflection

Two scenarios were assumed. One was exactly the same as the Park-2001 project that was a shallow excavation in clay with T-shape buttress walls with $L_w = 5$ m and $L_f = 2.5$ m. The other was similar to the Jinshan south road project but with R-shape buttress walls with $L_r = 5.6$ m. In each scenario, an analysis was performed with the assumption of no frictional resistance between the side surface of web of buttress walls and the adjacent soil.

Figure 12a shows the computed wall deflections for the deep excavation in sand with R-shape buttress walls. Results show that with consideration of frictional resistance between the buttress walls and the adjacent soil, the computed wall deflection was less than that without buttress walls. The computed wall deflection for frictionless case was almost the same as that without buttress walls. This implies that the main mechanism of R-shape buttress walls in reducing the wall deflection was due to the frictional resistance between buttress walls and the adjacent soil. The combined bending stiffness of the diaphragm wall from the diaphragm wall and the R-shape buttress wall plays insignificant role in the reduction in the wall deflection. This is because when the buttress walls were demolished along with the removal of soil, the buttress walls below the excavation bottom were mainly “pushed” by the diaphragm wall rather than providing the bending resistance against the deformation of the diaphragm wall.

Figure 12b shows the computed wall deflections for the shallow excavation in clay with T-shape buttress walls.

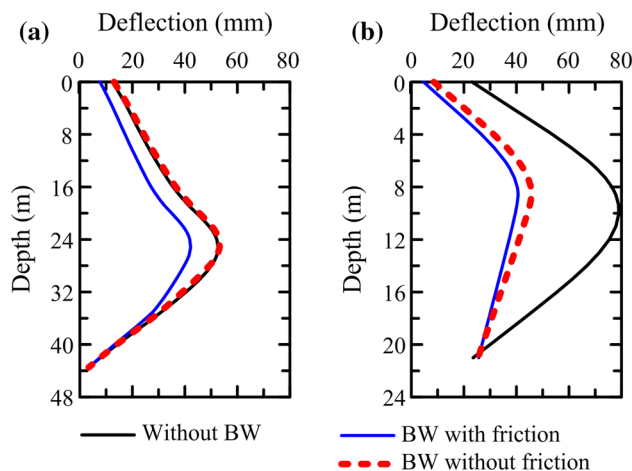


Fig. 12 Comparison of computed wall deflections for the cases of with buttress walls, without buttress walls, and with buttress walls but no friction **a** R-shape buttress wall in the deep excavation in sand; **b** T-shape buttress walls in the shallow in clay

Results show that the excavation with buttress walls was of less wall deflections than that without. The wall deflection for the scenario of no frictional resistance between the web surface of the buttress walls and the adjacent soil was much smaller than that of no buttress walls but slightly higher than that with frictional resistance. Since Fig. 12a has demonstrated that the combined bending stiffness from both diaphragm wall and buttress walls plays insignificant role in the reduction in the wall deflection, the reduction in wall deflection for the T-shape buttress walls mainly comes from the bearing resistance of the flange against the soil in front of the flange. For both with and without frictional resistance, the upper diaphragm wall, above the excavation bottom, deformed with curvature, but the lower diaphragm wall, below the excavation bottom, deflected with more close to the straight type. This is because the combined bending stiffness below the excavation bottom was sufficiently large that the wall moved laterally in a straight type rather than bending. Compared with the lower diaphragm wall, the bending stiffness of the upper diaphragm wall was relatively small so that it deformed with some curvature.

Similar phenomenon has been found in the deep excavation in clay and shallow excavation in sand.

4.2 Efficiency of R-shape buttress walls

As studied in the preceding section, the main restraining effect of R-shape buttress walls comes from the frictional resistance between buttress walls and adjacent soil when the buttress wall was demolished along with the removal of soil. This section will further study the efficiency of R-shape buttress walls with different lengths, in sand/clay, in the shallow/deep excavation.

Figure 13 shows the variation of the computed wall deflections for the scenarios with buttress walls where $L_r = 5, 10, 20$ m and without buttress walls, respectively. The amount of wall deflection certainly decreased with the increasing length of buttress walls in both shallow and deep excavations in sand or clay. Figure 14 shows the amount of reduction in terms of the MR value due to the installation of buttress walls, indicating that the longer L_r , the more reduction in the wall deflection. The reduction rate decreased as the buttress wall length increased. The MR value for the cases of buttress walls in sand had a better efficiency in reducing the wall deflection in both shallow and deep excavations.

To investigate the mobilization of shear strength, the relative shear stress ratio, τ_{rel} , is defined as the ratio of shear stress to the shear strength of a soil for a given effective normal stress. The $\tau_{rel} = 1.0$ implies that the soil adjacent to the buttress wall was at the failure state, and its shear strength or frictional resistance was fully mobilized. Figures 15 and 16 illustrate the variation of the maximum

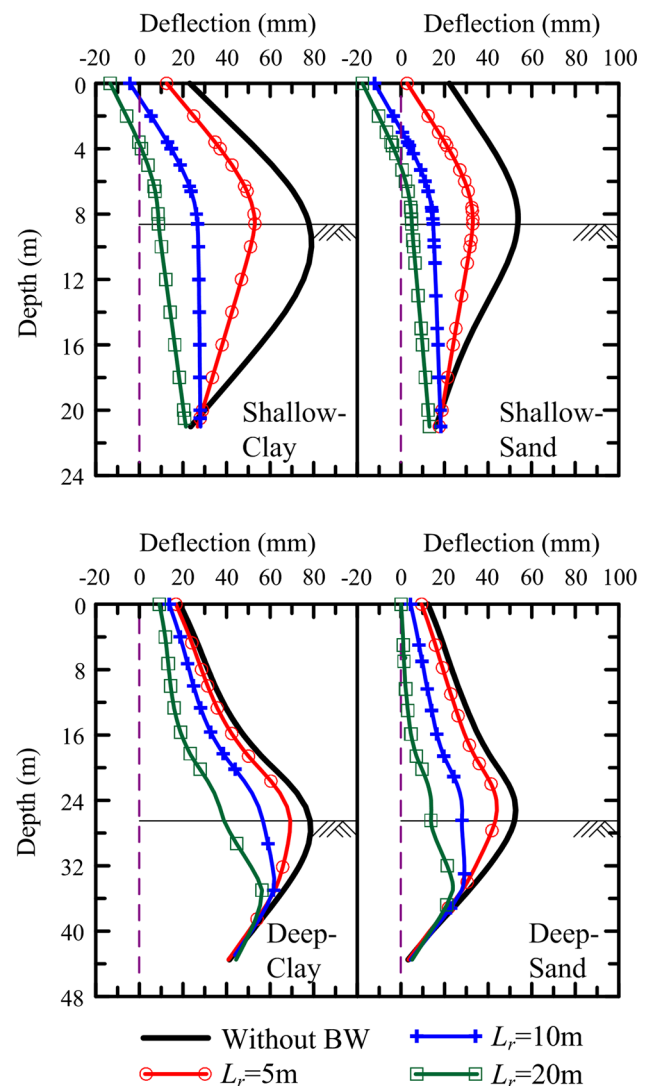


Fig. 13 Comparison of computed wall deflections for different lengths of R-shape buttress wall in the excavations

shear stress and relative shear stress ratio, respectively, on the surface of the buttress wall in the shallow excavation in clay and in sand, with the buttress wall length. Note that due to the boundary between different soil layers, the fluctuation of the shear stress and relative shear stress ratio distribution are found in Figs. 15 and 16 and the following similar figures. As shown in Fig. 15, the induced shear stress occurred at the diaphragm wall with the smallest value and increased with the increasing distance from the diaphragm wall. The τ_{rel} was also smallest near the diaphragm wall and generally increased with the increasing distance from the diaphragm wall, up to a value of 1.0. The τ_{rel} was mostly close to 1.0 for the short length of the buttress wall, e.g., $L_r = 5$ m, especially in clay and majorly much < 1.0 for the longer length of the buttress wall, e.g., $L_r = 20$ m, especially in sand (Fig. 16). Therefore, to further restrain the wall deflection, the length of buttress

wall needs to be increased in order to provide larger frictional resistance. Similar phenomena were also found in the deep excavation cases.

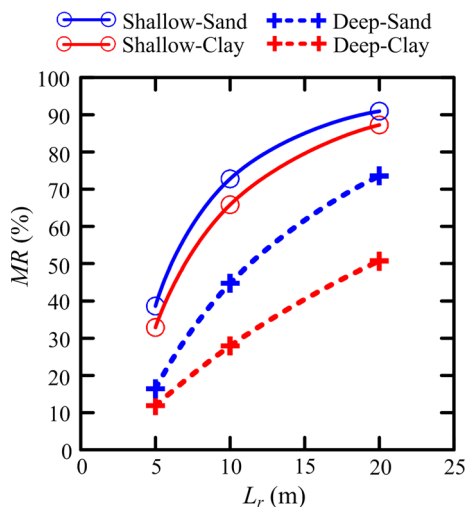


Fig. 14 Variation of the MR values with the length of R-shape buttress wall

Figure 14 also shows that the MR value in the shallow excavation was larger than that in the deep excavation in both sand and clay. The R-shape buttress wall in the shallow excavation seems to have a better effect than that in the deep excavation. This can be attributed to the fact that the τ_{rel} value in the deep excavation was generally higher than that in the shallow excavation under the same condition, the identical buttress wall length and same type of soil. The frictional resistance between the buttress wall and the adjacent soil was almost fully mobilized in the deep excavation due to the large shear stress induced at the early stage of excavation, and therefore, its τ_{rel} was mostly close to 1.0. Therefore, it was necessary to have a larger length and greater depth of the buttress walls in the deep excavation to obtain a better effect in reducing the wall deflection.

Figures 15 and 16 also show a relative small driving stress and relative shear stress ratio within the first 2.0 m from the diaphragm wall, no matter how long the buttress was. This phenomenon can be explained by the fact that the movement at any location of the buttress wall was all the same, almost the same as the movement of the diaphragm

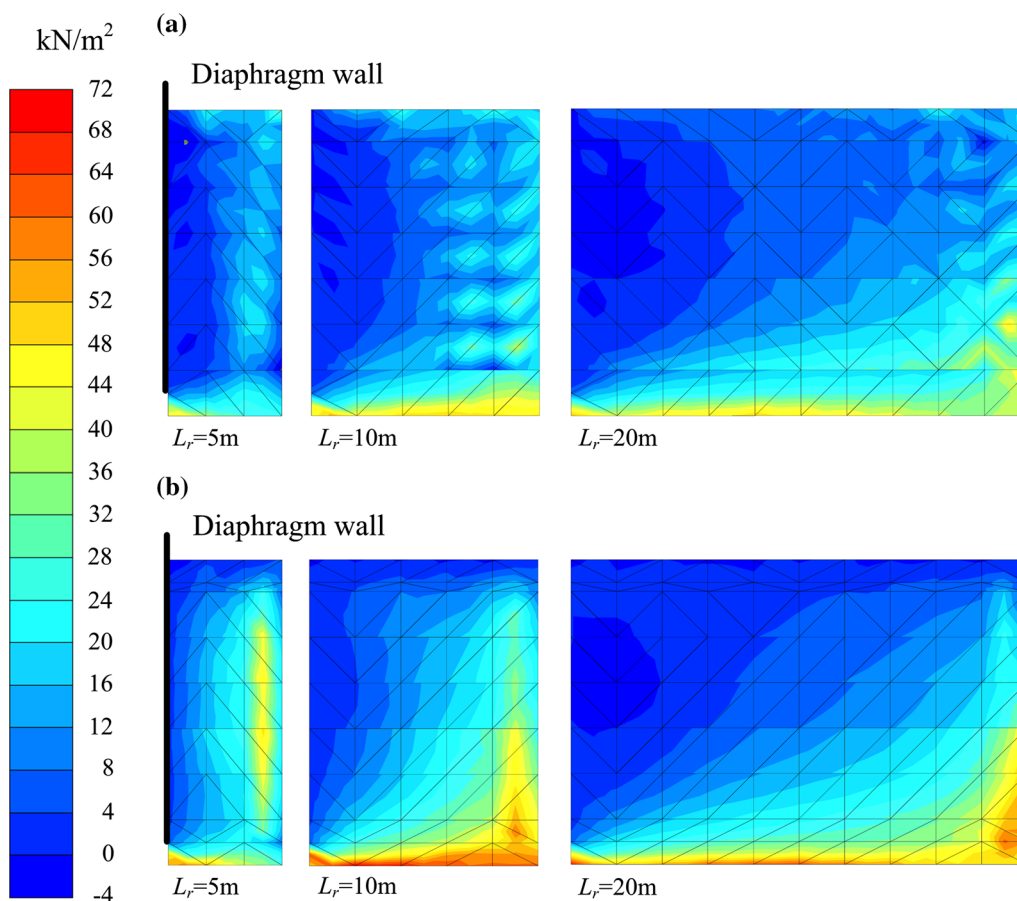


Fig. 15 Distribution of shear stress for the cases with different lengths of R-shape buttress wall **a** shallow excavation in clay; **b** shallow excavation in sand

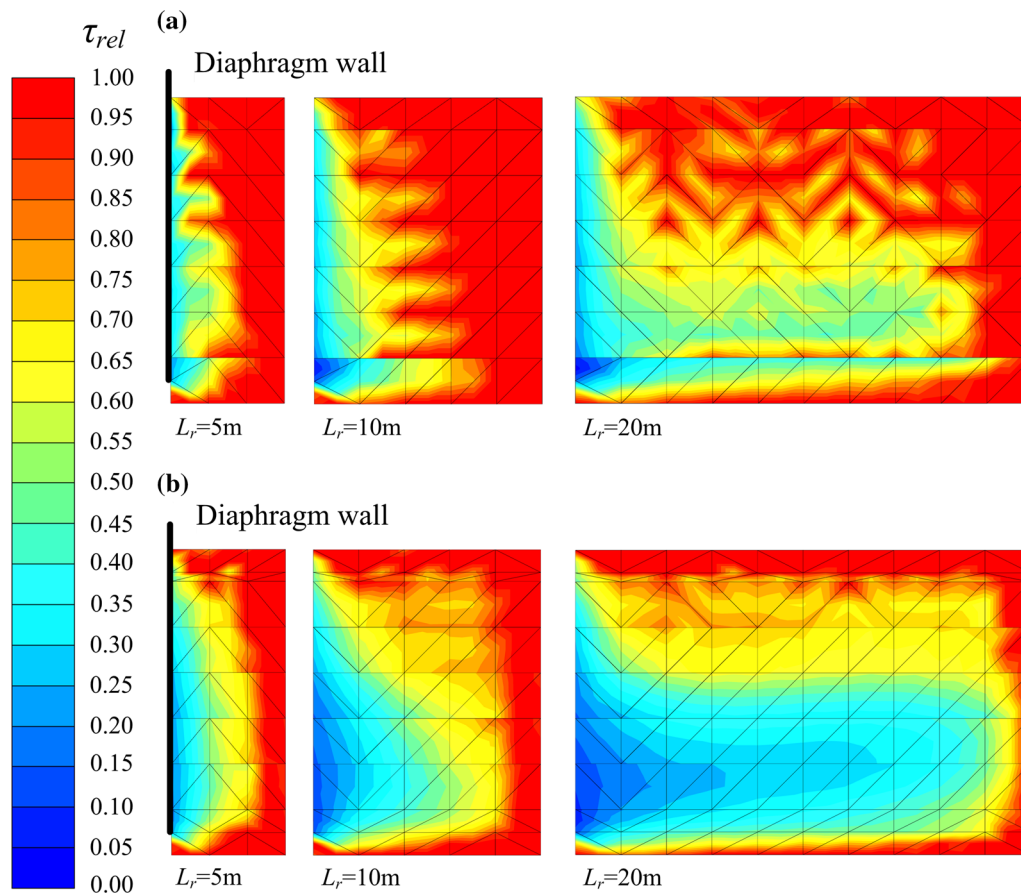


Fig. 16 Distribution of relative shear stress ratio for the cases with different lengths of R-shape buttress wall **a** shallow excavation in clay; **b** shallow excavation in sand

wall because the buttress wall had a very high axial stiffness. The soil in front of the diaphragm wall, say, 2.0 m from the diaphragm wall, directly pushed by the diaphragm wall, should have almost the same amount of movement as the diaphragm wall or buttress wall. Therefore, the relative displacement between the buttress wall and the soil within the first 2.0 m from the diaphragm wall was very small, but it increased gradually with the increasing distance from the diaphragm wall. The relative shear stress ratio was therefore very small near the diaphragm wall, and it increased with the increasing distance from the diaphragm wall. It was clear that if the buttress wall length was <2.0 m, the buttress wall was unable to restrain the wall deflection although the combined bending stiffness from the contribution of the diaphragm wall and buttress wall seems increased (Fig. 14).

4.3 Efficiency of T-shape buttress walls

As studied in the preceding section, the restraining effect for T-shape buttress walls comes from the frictional resistance between the buttress walls and adjacent soil and

bearing resistance from the flange. This section will further study the efficiency of T-shape buttress walls with different lengths of the web and flange in sand/clay, in the shallow/deep excavation. Three combinations of web length (L_w) and flange length (L_f) were adopted for analysis: $L_w = 5$ m and $L_f = 2.5$ m, $L_w = 5$ m and $L_f = 5$ m (i.e., L_f increases 2.5 m), $L_w = 7.5$ m (i.e., L_w increases 2.5 m) and $L_f = 2.5$ m.

Figure 17 shows the computed wall deflections for the above three combinations and case of without buttress walls in shallow/deep excavations in sand/clay. The MR values corresponding to Fig. 17 are summarized as listed in Table 5. Compared with the wall deflection for $L_w = 5$ m and $L_f = 2.5$ m, either increase in the web length up to 7.5 m or flange length up to 5.0 m can reduce the wall deflection. Similar to the R-shape buttress wall, either the T-shape buttress wall in sand or in the shallow excavation has a better reduction in the wall deflection than that in clay or deep excavation.

Figure 18 shows the τ_{rel} on the web surface of the T-shape buttress wall in the shallow excavation in clay and in sand, with three combinations of web and flange lengths.

As shown in this figure, the τ_{rel} was very small both near the diaphragm wall and near the flange. The former was similar to the R-shape buttress wall, and the latter was due to the restraint by the flange because the movement of the

soil adjacent to the web was constrained by both the diaphragm wall and the flange, and thus, the τ_{rel} on the T-shape buttress wall was generally smaller than that on the R-shape, comparing Figs. 16 and 18. The phenomenon seems to be more obvious as the flange length increased by comparing the τ_{rel} in the case of $L_w = 5$ m and $L_f = 2.5$ m with that of $L_w = 5$ m and $L_f = 5$ m. Though the τ_{rel} or frictional resistance on the web in the case of $L_w = 5$ m and $L_f = 5$ m decreased, the bearing resistance of the flange increased and the resulting overall efficiency increased, as demonstrated in Fig. 17 and Table 5.

As observed in Fig. 18, the τ_{rel} on the web surface for the case of $L_w = 7.5$ m and $L_f = 2.5$ m was larger than that of the case of $L_w = 5$ m and $L_f = 2.5$ m. The τ_{rel} was less influenced by the diaphragm wall and flange when the web length increased. Therefore, increase in the web length can provide more frictional resistance and the wall deflection reduced as a result.

It is clear that either extension of the web length or increase in the flange length can reduce the wall deflection. Under a condition of identical length/area of buttress wall, increase in the web length has a slightly better effect in reducing the wall deflection than extension of the flange length as shown in Fig. 17 and Table 5 by comparing the case of $L_w = 7.5$ m and $L_f = 2.5$ m with the case of $L_w = 5$ m and $L_f = 5$ m. The phenomenon can be explained by the fact that the frictional resistance can be mobilized at a relatively small displacement while the bearing resistance required a relatively large displacement to be mobilized. Extension of the flange length can increase the bearing resistance that may not be fully mobilized, while it would reduce the frictional resistance of the web. The overall efficiency of increase in the flange length was therefore less than increase in the web length.

Similarly, the characteristics of T-shape buttress walls in deep excavations in sand/clay also have a similar behavior to the shallow excavation. Figure 17 also shows the variation of wall deflections of the deep excavation in sand and clay with different combinations of T-shape buttress walls, and their MR values are also summarized in Table 5.

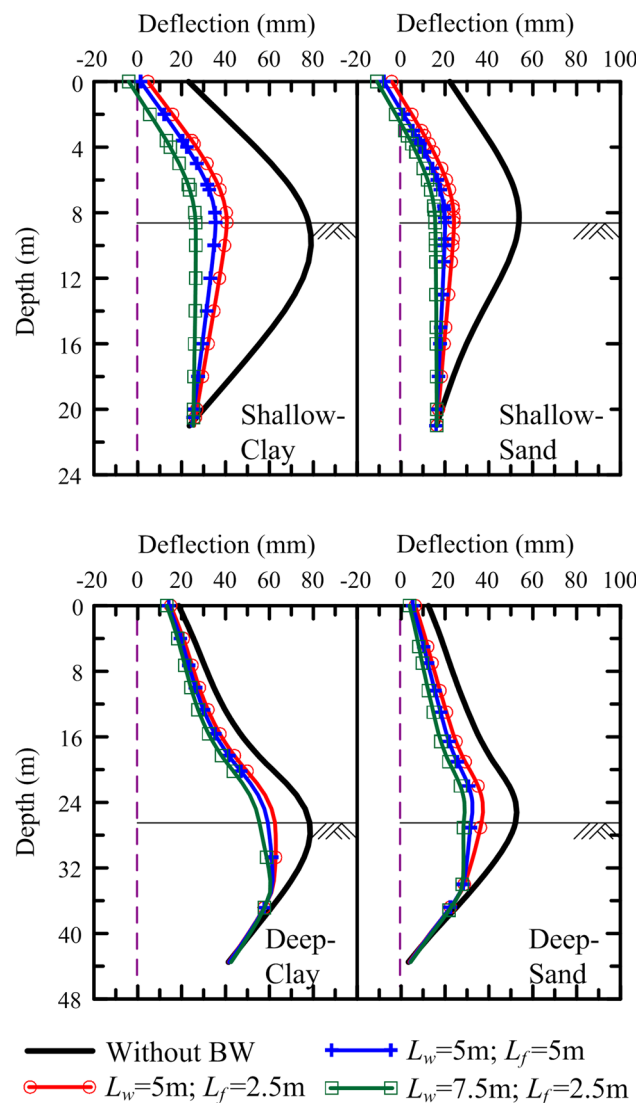


Fig. 17 Comparison of the wall deflections for the cases with T-shape buttress wall with different web and flange lengths

Table 5 Comparison of the MR values for R-shape and T-shape buttress walls

L_w, L_f (m)	L_r (m)	MR (%)	T-shape				R-shape			
			Shallow-Clay	Shallow-Sand	Deep-Clay	Deep-Sand	Shallow-Clay	Shallow-Sand	Deep-Clay	Deep-Sand
			5, 2.5	–	48.6	55.2	19.9	29.2	–	–
5, 5	–	55.1	62.8	21.8	38.4	–	–	–	–	
7.5, 2.5	–	66.5	71.3	23.1	45.0	–	–	–	–	
–	5.6	–	–	–	–	37.0	43.9	14.0	20.1	
–	7.5	–	–	–	–	51.4	58.8	18.4	30.0	

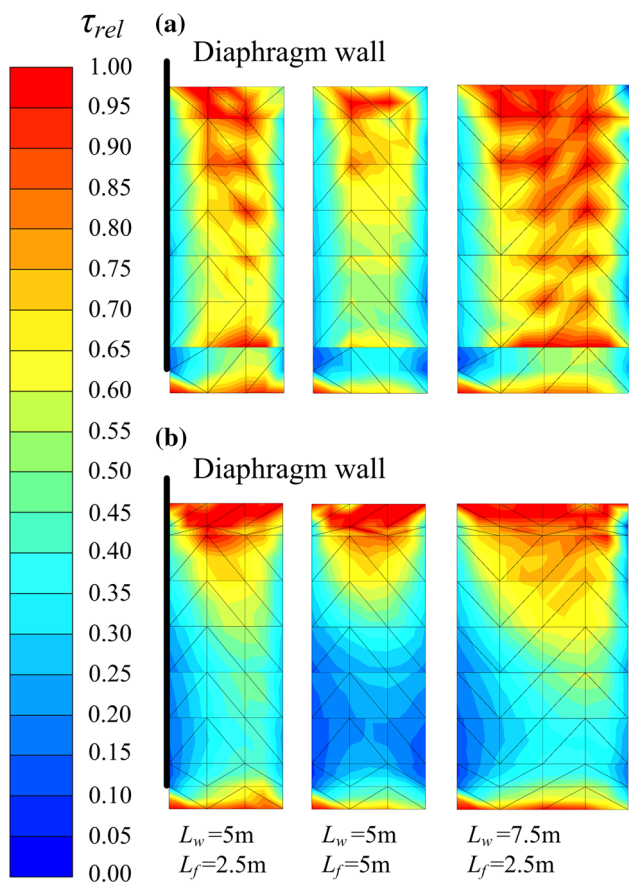


Fig. 18 Distribution of the relative shear stress ratio of the web of T-shape buttress walls in the shallow excavation **a** in clay; **b** in sand

5 Discussion

As studied in the previous sections, both R-shape and T-shape buttress walls can provide additional resistance against the movement of the diaphragm wall. Assuming that buttress walls were all 0.6 m in thickness, the computed wall deflections for the cases of T-shape with $L_w = 5$ m and $L_f = 2.5$ m, R-shape with $L_r = 5.6$ m and R-shape with $L_r = 7.5$ m are adopted for study. Among these cases, the case of T-shape with $L_w = 5$ m and $L_f = 2.5$ m was of the same distance from the end of the buttress wall to the diaphragm wall as the case of R-shape with $L_r = 5.6$ m. The case of T-shape with $L_w = 5$ m and $L_f = 2.5$ m has the same total length/area as the case of R-shape with $L_r = 7.5$ m.

As listed in Table 5, the case of T-shape with $L_w = 5$ m and $L_f = 2.5$ m had a larger MR value than the case of R-shape with $L_r = 5.6$ m for both deep and shallow excavations in sand/clay. This implies that with the same distance from the end of the buttress walls to the diaphragm wall, the T-shape buttress wall had a better effect in reducing the wall deflection than the R-shape. This is because the flange also provides an additional bearing

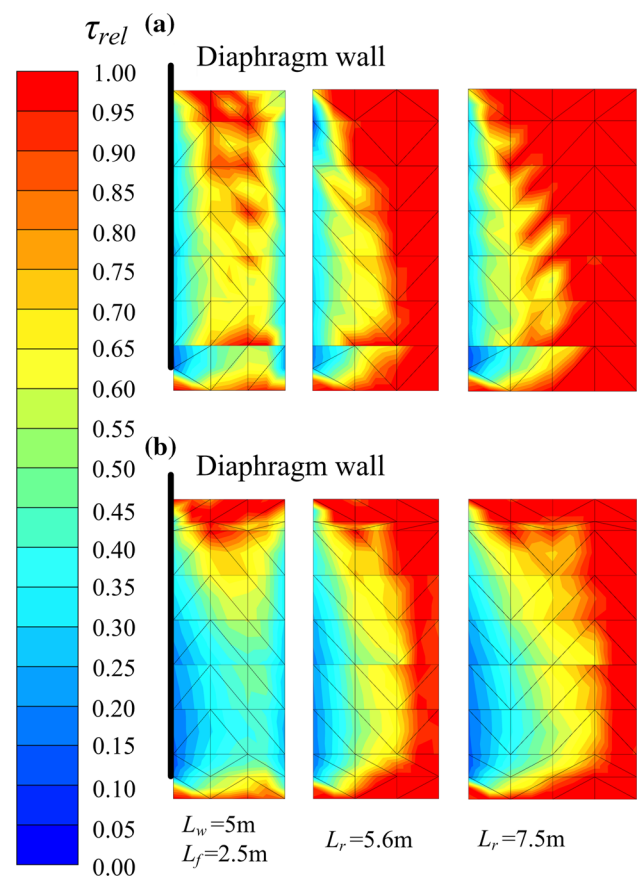


Fig. 19 Comparison of the relative shear stress ratio between the web of T-shape and the R-shape buttress walls for shallow excavation **a** in clay; **b** in sand

resistance though the mobilized frictional resistance of the web was smaller than the R-shape, as shown in Fig. 19. A similar phenomenon has been found in the deep excavation in sand/clay.

Table 5 also exhibits that the case of R-shape with $L_r = 7.5$ m was of the larger MR value than the case of T-shape with $L_w = 5$ m and $L_f = 2.5$ m in the shallow excavation in sand/clay where these two cases had the same length/area of buttress walls. However, in the deep excavation, the MR values were almost the same for both R-shape and T-shape, and their values were much smaller than those in the shallow excavation. As shown in Fig. 19, the τ_{rel} for the case of R-shape with $L_r = 7.5$ m was much higher than the case of T-shape with $L_w = 5$ m and $L_f = 2.5$ m in the shallow excavation in sand/clay. With the same length/area of the buttress walls, the overall mobilized frictional resistance of the R-shape buttress wall was higher than the sum of the mobilized frictional resistance of the web and bearing resistance, less mobilized, of the flange because the wall deflection was not sufficiently large. The similar trend was also found in the deep excavation, but relatively large wall deflections caused the full

mobilization of the bearing resistance of the flange as well as the full mobilization of the frictional resistance of the web, and therefore, their MR values were much smaller. The difference of the overall resistance between the R-shape and T-shape buttress walls thus became very small, resulting in almost the same MR values.

Moreover, the case studies demonstrated that the Park-2001 project, a shallow excavation in clay with the T-shape buttress wall, had a larger MR value than the Jinshan south road project, a deep excavation in sand with the R-shape buttress wall. It seems that the T-shape buttress wall had a better efficiency in reducing the wall deflection. As listed in Table 5 and discussed before, buttress walls in the shallow excavation had a better efficiency than that in the deep excavation though buttress walls in clay provide a less restraining effect than that in sand. Moreover, the T-shape buttress walls in the Park-2001 project were adopted with $L_w = 5$ m and $L_r = 2.5$ m. Such a dimension of the T-shape buttress wall was equivalent to the R-shape with $L_r = 7.5$ m in terms of the restraining effect, as studied previously. The R-shape buttress walls with $L_r = 2.5$ m in the Jinshan south road project were constructed between GL +0 and GL -20.2 m and with $L_r = 5$ m between GL -20.2 and GL -35 m. Their effects should be much smaller than the equivalent T-shape dimension, $L_r = 7.5$ m. Moreover, $L_r = 2.5$ m would cause the soil adjacent to the buttress wall moving together with the buttress wall. The frictional resistance was not sufficiently mobilized, and therefore, its effect was not as good as that in the Park 2001 project.

6 Conclusions

Based on the studies in this paper, the following conclusion can be drawn:

1. When buttress walls in excavations were demolished along with excavation of soil, the effect of reduction in the wall deflection mainly came from the frictional resistance between the side surface of buttress walls and adjacent soil rather than from the combined bending stiffness contributing from the diaphragm wall and buttress walls.
2. When the short length of buttress walls was adopted, for example, 2.0 m, the soil adjacent to the buttress walls will almost have the same amount of movement as the buttress walls, causing the frictional resistance between the buttress walls and adjacent soil being little mobilized. Therefore, it would be unable to reduce the wall deflection effectively.
3. The main mechanism of the R-shape buttress wall was due to the frictional resistance. The amount of reduction in wall deflection increased with the increasing length of the buttress wall.
4. Though the T-shape buttress wall was with the bearing resistance from the flange, the movement of the soil adjacent to the web was constrained by both the diaphragm wall and the flange, causing a smaller mobilized frictional resistance. Such a phenomenon increased with the increasing flange length. Increase in the web length had a slightly better effect in reducing the wall deflection than that of the flange length.
5. Under a condition of the same amount of length/area of buttress walls, the R-shape buttress wall had a better effect than the T-shape buttress wall. When the excavation went deeper, the difference between the R-shape and T-shape became smaller.
6. Buttress walls in sand, no matter in shallow or deep excavations, can provide more resistance against the movement of the diaphragm wall than that in clay.
7. In the deep excavation, the frictional resistance from the buttress wall was almost fully mobilized at early or intermediate stages of excavation. The buttress walls thus provide less resistance at the final stage. Therefore, to effectively reduce the wall deflection in deep excavations, longer and deeper buttress walls were generally recommended.

Acknowledgments The authors acknowledge the support provided by the Ministry of Science and Technology in Taiwan via Grant No. MOST103-2221-E-146 -004.

References

1. ACI Committee 318 (1995) Building code requirements for structural concrete (ACI 318-95) and commentary (ACI 318R-95). American Concrete Institute (ACI), Farmington Hills
2. Bolton MD (1986) The strength and dilatancy of sands. *Geotechnique* 36(1):65–78
3. Calvello M, Finno R (2004) Selecting parameters to optimize in model calibration by inverse analysis. *Comput Geotech* 31(5):410–424
4. Chen SL, Ho CT, Li CD, Gui MW (2011) Efficiency of buttress walls in deep excavations. *J GeoEng* 6(3):145–156
5. Comodromos EM, Papadopoulou MC, Konstantinidis GK (2013) Effects from diaphragm wall installation to surrounding soil and adjacent buildings. *Comput Geotech* 53:106–121
6. Deng WB (2013) The effect of buttress walls on wall deflection in deep excavation. National Taiwan University of Science and Technology, Master's Thesis (in Chinese)
7. Duncan JM, Chang CY (1970) Nonlinear analysis of stress and strain in soils. *J Soil Mech Found Div* 96(5):637–659
8. Gaba AR (1990) Jet grouting at Newton station. In: Proceedings of the 10th Southeast Asia geotechnical conference, Taipei, pp 77–79
9. Hsieh HS, Lu LC (1999) A note on the analysis and design of diaphragm wall with buttresses. *Sino-Geotechnics* 76:39–50 (in Chinese)

10. Hsieh HS, Wu LH, Lin TM, Cherng JC, Hsu WT (2011) Performance of T-shaped diaphragm wall in a large scale excavation. *J GeoEng* 6(3):135–144
11. Hsieh PG, Ou CY, Lin YL (2013) Three dimensional numerical analysis of deep excavations with cross walls. *Acta Geotech* 8(1):33–48
12. Hsieh PG, Ou CY, Lin YK, Lu FC (2015) Lessons learned in design of an excavation with the installation of buttress walls. *J GeoEng* 10(2):25–35
13. Hwang RN, Moh ZC, Wang CH (2007) Performance of wall systems during excavation for core pacific city. *J GeoEng* 2(2):53–60
14. Jaky J (1944) The coefficient of earth pressure at rest. *J Soc Hung Archit Eng* 78(22):355–358
15. Khoiri M, Ou CY (2013) Evaluation of deformation parameter for deep excavation in sand through case histories. *Comput Geotech* 47(1):57–67
16. Ladd CC, Foott R, Ishihara K, Schlosser F, Poulos HG (1977) Stress-deformation and strength characteristics. In: *Proceedings of the 9th international conference on soil mechanics and foundation engineering*, vol 2. Tokyo, pp 421–494
17. Lim A, Ou CY, Hsieh PG (2010) Evaluation of clay constitutive models for analysis of deep excavation under undrained conditions. *J GeoEng* 5(1):9–20
18. Liu GB, Ng CWW, Wang ZW (2005) Observed performance of a deep multistrutted excavation in Shanghai soft clays. *J Geotech Geoenviron Eng* 131(8):1004–1013
19. Ng CWW, Yan WM (1999) Three-dimensional modeling of a diaphragm wall construction sequence. *Geotechnique* 49(6):825–834
20. Ou CY, Shiau BY (1998) Analysis of the corner effect on the excavation behavior. *Can Geotech J* 35(3):532–540
21. Ou CY, Chiou DC, Wu TS (1996) Three-dimensional finite element analysis of deep excavation. *J Geotech Eng* 122(5):337–345
22. Ou CY, Liao JT, Lin HD (1998) Performance of diaphragm wall constructed using top-down method. *J Geotech Geoenviron Eng* 124(9):798–808
23. Ou CY, Hsieh PG, Lin YL (2011) Performance of excavations with cross walls. *J Geotech Geoenviron Eng* 137(1):94–104
24. Ou CY, Hsieh PG, Lin YL (2013) A parametric study of lateral wall deflections in deep excavations by the installation of cross walls. *Comput Geotech* 50:55–65
25. Parashar S, Mitchell R, Hee MW, Sanmugathan D, Sloan E, Nicholson G (2007) Performance monitoring of deep excavation at Changi WRP project. In: *Proceedings of the 7th international symposium on field measurements in geomechanics*. Singapore, pp 1–12
26. PLAXIS 3D (2013) Computer software. PLAXIS, Delft
27. Poh TY, Wong IH (1998) Effects of construction of diaphragm wall panels on adjacent ground: field trial. *J Geotech Geoenviron Eng* 124(8):749–756
28. Schanz T, Vermeer PA, Bonnier PG (1999) The hardening soil model—formulation and verification. In: *Brinkgreve RBJ (ed) Beyond 2000 in computational geotechnics*. Balkema, Rotterdam, pp 281–296
29. Wong KS, Wong IH, Broms BB (1987) Methods of improving the stability of deep excavations in soft clay. In: *Proceedings of the 8th Asian regional conference on soil mechanics and foundation engineering*. Kyoto, pp 321–324